Glass Physics and Chemistry, Vol. 31, No. 4, 2005, pp. 439–451.

PROCEEDINGS OF THE TOPICAL MEETING OF THE EUROPEAN CERAMIC SOCIETY "NANOPARTICLES, NANOSTRUCTURES, AND NANOCOMPOSITES"

(St. Petersburg, Russia, July 5–7, 2004)

System Approach to Analysis of the Role of the Synthesis Components and Stability of the MCM-41 Mesostructured Silicate Material

S. D. Kirik, O. V. Belousov, V. A. Parfenov, and M. A. Vershinina

Institute of Chemistry and Chemical Technology, Siberian Division, Russian Academy of Sciences, ul. Karla Marksa 42, Krasnoyarsk, 660049 Russia

Abstract—The formation of a mesostructured silicate material of the MCM-41 type is studied. The influence of the replacement of components in a reaction medium is investigated experimentally. Analysis of the results obtained and the data available in the literature suggests that the process under investigation is based on the approximate stoichiometric supramolecular interaction between $[Si_4O_{4+x}(OH)_{9-x}]^{-(1+x)}$ silicate polyanions and $C_{16}H_{33}(CH_3)_3N^+$ cetyltrimethylammonium cations with the formation of supramolecular aggregates, which condense to a mesostructured organosilicate composite. A further evolution of the product involves hydrolysis of the inner surface and the polymerization of the inorganic component. It is demonstrated that the properties of the product are determined, to a large extent, by the components of the reaction medium, which control the relative reaction rates in the process. The inference is made that an alcohol–ammonia medium is the most optimum for alkaline synthesis. This medium provides good preparation of the initial components for the reaction and the high rate of hydrolysis of pore walls, minimizes the osmotic effects during hydrothermal treatment, and, eventually, favors the formation of a highly structured hydrothermally stable material.

INTRODUCTION

The wide variety of silica species described by Iler in his well-known monograph [1] is associated with the easy formation of metastable states that have close energies, are stable in time, and arise from a set of parallel, reversible and irreversible, competitive processes during the evolution of a product. Although the chemical composition of such systems is relatively simple, there is little point in believing that their behavior can be thermodynamically and kinetically described in detail. More likely, researchers use a set of empirical reasonable intuitive notions rather than correct concepts. A prominent example of such a situation is provided by the modern history of research into mesostructured mesoporous silicates.

There is no doubt about the joint priority of scientists of the Mobil Research and Development Co. [2, 3] and Japanese researchers [4], who, in the early 1990s, for the first time systematically investigated the synthesis, structure, and properties of mesostructured mesoporous silicates belonging to the M41S and FSU families. However, it should be noted that a number of data for similar materials were obtained far in advance of those reported in the above works. In particular, a strong flocculating effect of small additives of cetyltrimethylammonium chloride on silica sols with the formation of lamellar aggregates was described in 1957 [5]. More recently, Chiola *et al.* [6] observed a similar phenomenon. However, all researchers before publishing the works [2, 3] could not recognize the significance of the prepared compounds, and their unique properties governed by the crystallographically ordered (on a nanoscale) porous structure with a pore surface up to 1000 m^2/g were not studied in depth.

Ten-year investigations of mesostructured silicate materials have revealed radically new promising potentialities of liquid-crystal templating for preparing new inorganic materials [7–16]. The interaction of surface-active organic molecules with inorganic polyanions under specific conditions leads to the formation of supramolecular particles condensed from a solution to a mesastructured mesophase with a structure formed according to the laws of liquid-crystal media. The resulting composite consists of regularly alternating organic and inorganic regions. The nontraditional term "mesophase" (whose meaning is not universally accepted) is used because the nature of compounds themselves corresponds to a boundary between organic and inorganic materials, on the one hand, and the product is in the state of an active evolution, on the other hand. Hydrothermal treatment in an autoclave (for the most part, resulting in polymerization of the inorganic component) and subsequent burning of the organic component in air at temperatures above 300°C lead to the formation of the mesostructured mesoporous material, which, as judged from the chemical composition,

1087-6596/05/3104-0439

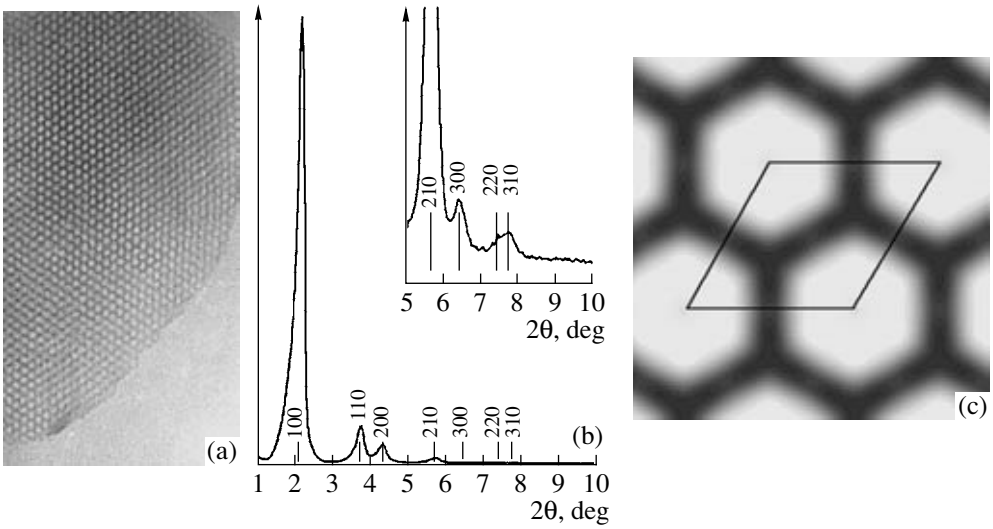

Fig. 1. (a) Electron microscope image [17], (b) X-ray diffraction pattern, and (c) electron density map obtained from the X-ray diffraction pattern [18] for the MCM-41 mesostructured mesoporous silicate material.

is an inorganic polyanion that has a geometrically regular surface with a very large area.

The silicate material, historically referred to as MCM-41 [2, 3], has been most thoroughly investigated to date. Figure 1 shows the electron microscope image (Fig. 1a) [17], the X-ray diffraction pattern (Fig. 1b), and the electron density map (Fig. 1c) obtained from the X-ray diffraction pattern [18] for the MCM-41 mesostructured silicate material. The researchers of the Mobil, who obtained this material for the first time, described a rather large number of initial reagents that allow one to prepare the mesostructured material. Organosilicon compounds (tetramethyl orthosilicate, tetraethyl orthosilicate, etc.), different products of colloidal silica, and soluble silicates were proposed to use as a silica source. Surface-active agents (SAA) belonging to the class of quaternary ammonium compounds, for example, alkyltrimethylammonium hydroxide, and salts of these compounds can serve as structuring agents. Specifically, compounds with C_{12}–C_{22} alky chains are used for the MCM-41 materials. The most popular structuring agent is the $C_{16}H_{33}(CH_3)_3NBr$ cetyltrimethylammonium bromide surfactant or other salts with the same cation. A number of organic compounds, such as mesitylene and different alcohols, are introduced into a reaction mixture as additional components [2]. The pH value of the medium is maintained by ammonia solutions, quaternary methylammonium or ethylammonium hydroxides, sodium hydroxide, sulfuric and acetic acids, etc.

A large number of combinations and concentration ratios of components, variants of their interactions, and stages and conditions of synthesis have been described in the literature. In all cases, the interaction results in the formation of mesostructured porous products, which can differ in structural perfection and other characteristics. A great deal of information is available in the literature. For example, the variation in the SAA/SiO_2 molar ratio over a wide range from 0.08 to 2.0 was analyzed in [10, 19]. However, specific features of synthesis procedures not only have been described in insufficient detail but have appeared to be somewhat incorrect in many cases. Most likely, this circumstance explains the absence of a comprehensive review of different variants for synthesizing materials with the analysis of chosen compositions. By disregarding business factors, it should be noted that clear concepts regarding the role of components and their reactivity in the processes under consideration, as well as a general concept of the mechanism of processes responsible for the formation of materials, have not been offered up to now. This problem has become topical, because a large number of works have been concerned with applications of mesostructured mesoporous materials. The requirements to the reproducibility, the stability in different media, the reactivity of the inner surface, and the morphology have been the focus of attention [19–23]. One of the goals of the present work was to examine the reproducibility of geometric characteristics of pores and their arrangement. Even when the synthesis procedure is repeated carefully, the lattice parameter can vary by 1 Å and more. Moreover, even larger variations in the lattice parameter can be observed after hydrothermal treatment and annealing. The stability of materials in corrosive media, in particular, the hydrothermal stability, is the most acute problem [8, 11, 24–28]. It was found that many MCM-41 samples are stable at high temperatures but do not withstand boiling in water [25, 26], they lose a mesostructure and transform into an amorphous state. However, Yu *et al.* [24], Kruk *et al.* [25], and Mokaya [29] succeeded in preparing hydrothermally stable materials. Researchers have directed their efforts toward finding the methods for eliminating

the above disadvantage. Attempts have been made to solve this problem by using the so-called salt effect [27, 30–33], coating pore walls with organosilicon compounds [28, 34, 35], increasing the thickness of pore walls in the course of hydrothermal treatment [23], and preparing element silicate materials with other elements [16, 29]. Undeniably, solving hydrothermal stability problem provides a way of extending the field of application of these promising materials.

In our opinion, the aforementioned situation is associated with the fact that all processes occurring in the course of material preparation and their duration are difficult to take into account and a detailed mechanism of formation of compounds, their molecular structure, and the role played by different components of a reaction medium in these processes are poorly understood.

In the works devoted to the problem of stability [8, 11, 24–28, 30–33], it has been repeatedly shown that the hydrothermal stability of MCM-41 samples prepared in amine or ammonia media is higher than the stability of similar samples synthesized in water–alcohol media. The products in both cases are characterized by a high structural ordering, and materials with the most perfect structure of a silicon–oxygen framework have been prepared in alkaline media [18, 36, 37]. Therefore, the quality of materials is affected by medium components that do not enter into the composition of the final product.

The aim of the present work was to elucidate the role of different components in the synthesis. For this purpose, we performed a series of experiments on sequential replacement of functional components in such a way as to change over from an alcohol–ammonia medium to a water–alkali medium. It is evident that a simple replacement of one component by another component does not lead to the formation of a material with optimum properties. In order to attempt to reveal the role of a particular component, we determined qualitative changes in the structural ordering due to the replacement of this component by another component. The structural ordering of a material was determined by X-ray diffraction analysis at each stage of its preparation, namely, after condensation, hydrothermal treatment, calcination, and test for the hydrothermal stability.

SAMPLE PREPARATION AND EXPERIMENTAL TECHNIQUE

The materials under investigation were prepared from the following initial reagents: cetyltrimethylammonium bromide $C_{16}H_{33}(CH_3)_3NBr$ (*CTA*Br, Aldrich, no. 85.582-0), tetraethoxysilane $Si(C_2H_5O)_4$ (*TEOS*, analytical grade), sodium silicate $Na_2SiO_3 \cdot 9H_2O$ (REAKhIM), ammonia NH_3 (13.4 *M*, $\rho = 0.905$ g/cm^3, analytical grade), sodium hydroxide NaOH (analytical grade), ethanol *Et*OH (96 wt %, rectified), and concentrated sulfuric acid H_2SO_4 (analytical grade). The stoichiometric ratios of the components used in the synthesis are presented in Figs. 2–7.

Cetyltrimethylammonium bromide was dissolved in water or a water–alcohol solution at room temperature with stirring for 30 min. The pH value of the surfactant solution was provided by adding an ammonia or NaOH solution. Tetraethoxysilane was added dropwise to the surfactant solution or the preliminarily prepared sodium silicate solution with vigorous stirring on a magnetic agitator. Introduction of the silicon-containing component almost immediately results in the hydrolysis, turbidity, and the formation of a suspension. The pH value of the medium was equal to 12.5 prior to introduction of tetraethoxysilane and 11.5 within 10 min after introduction. In this work, the time during which the product was formed was limited by 2 h. Then, the major portion of the product with a mother solution was placed in a Teflon autoclave in order to perform hydrothermal treatment at a temperature of 110°C for 2 h. A small portion of the product (for the test) was separated by filtering, washed with water to the neutral pH value of washed waters, and dried in air at room temperature. The same procedure was used for separating the product after hydrothermal treatment. Thereafter, the material was subjected to calcination in air at 550°C. The heating rate during calcination was equal to 3 K/min, and the calcination time at the final temperature was 3 h. In a number of experiments, the sodium silicate was used as the silicon source. In these experiments, the required pH value was ensured by acidification with a sulfuric acid solution.

The test for the stability was carried out by holding the material in water heated on a water bath at the boiling temperature for 2 h, followed by the examination of the change in the X-ray diffraction patterns.

After condensation, hydrothermal treatment, calcination, and test stages, portions of the material were withdrawn for X-ray diffraction analysis. The X-ray diffraction patterns were recorded on a DRON-4 automated diffractometer (CuK_α radiation, graphite monochromator, reflected beam). At small angles, the standard optical scheme of the diffractometer was complemented by a collimation slit (0.25 mm) in a primary beam at a distance of 90 mm from a tube focus and a modified Soller slit (the distance between plates was equal to 0.2 mm). Scanning was performed in the angular range $2\theta = 1°–7°$ with a step of 0.04° and an accumulation time of 10 s per point.

RESULTS AND DISCUSSION

Figures 2–7 show the X-ray diffraction patterns of the analyzed products at different stages of the evolution. The evolution of the product with the optimum set of the components for the alcohol–ammonia synthesis (Fig. 2) is not accompanied by a substantial change in the lattice parameter. The largest jump (increase) in the parameter a by approximately 1.5 Å is observed after

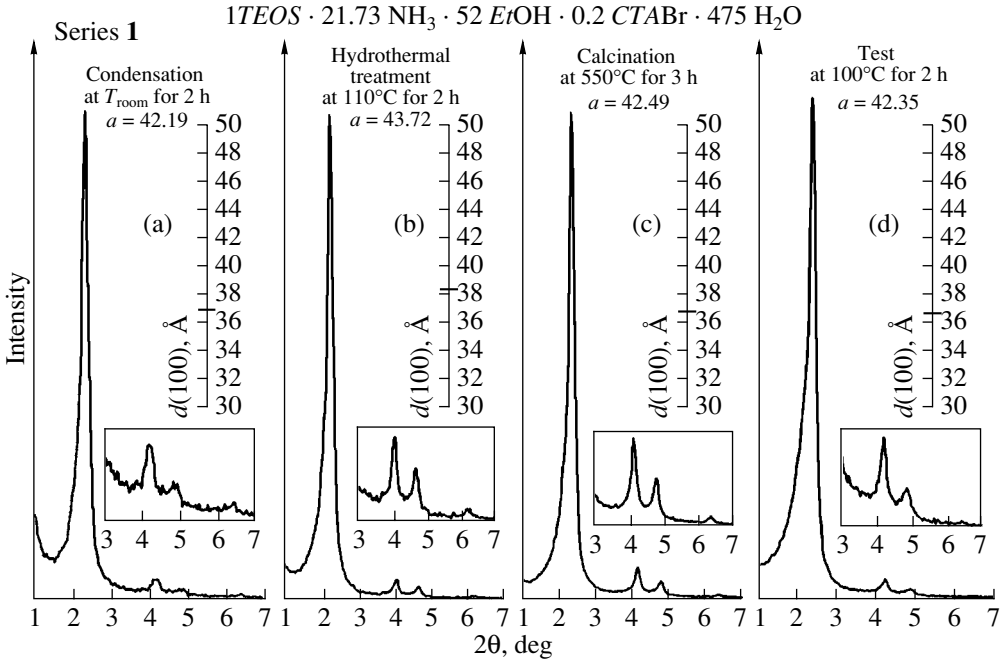

Fig. 2. X-ray diffraction patterns of products of series **1**. The interplanar distances corresponding to the most intense line are shown. Wherever possible, the lattice parameters are calculated.

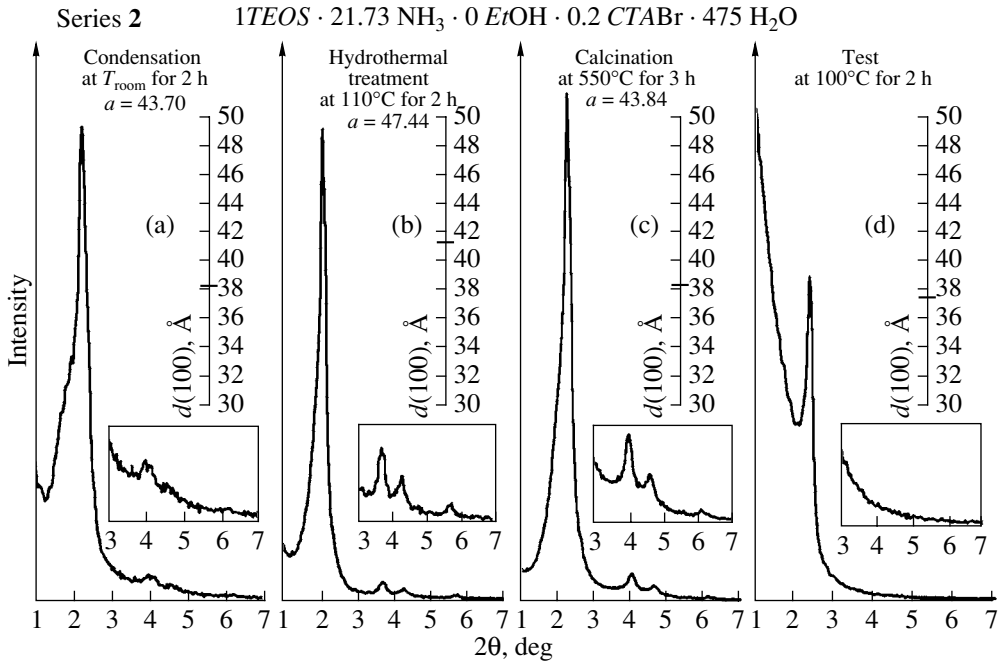

Fig. 3. X-ray diffraction patterns of products of series **2** (see capture to Fig. 2).

hydrothermal treatment. However, after calcination, the material virtually regains its initial structure. Boiling in water does not result in a noticeable change in the lattice parameter. The X-ray diffraction pattern contains as large as five peaks. Immediately after condensation, the product is quite perfect. However, the X-ray diffraction pattern involves indications that the framework is inhomogeneous: the (100) line has a weak shoulder, and the (110) and (200) peaks are smoothed. Hydrothermal treatment leads to a more homogeneous struc-

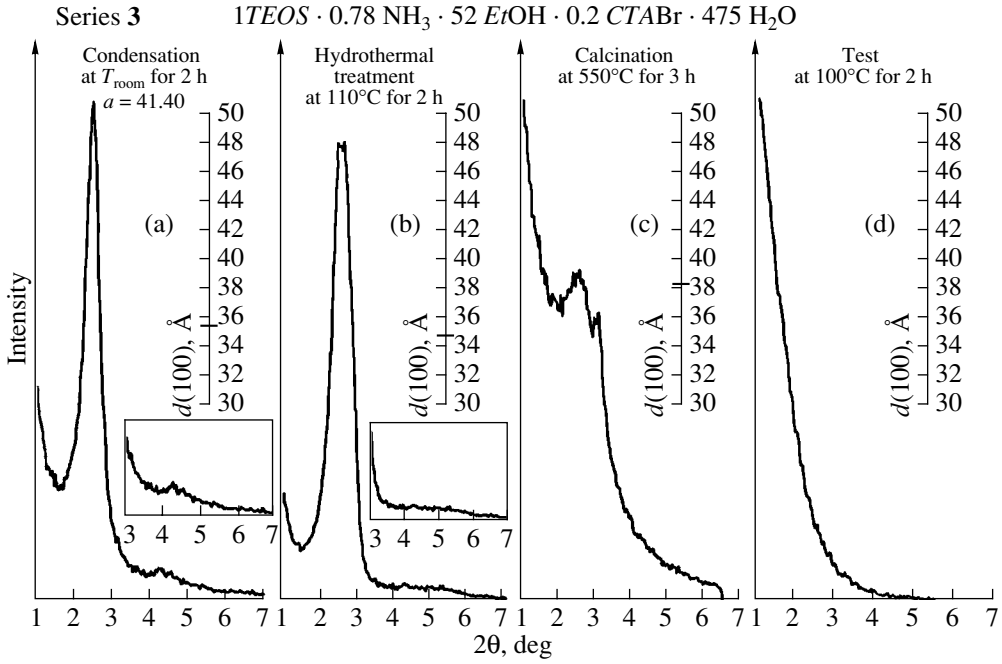

Fig. 4. X-ray diffraction patterns of products of series **3** (see capture to Fig. 2).

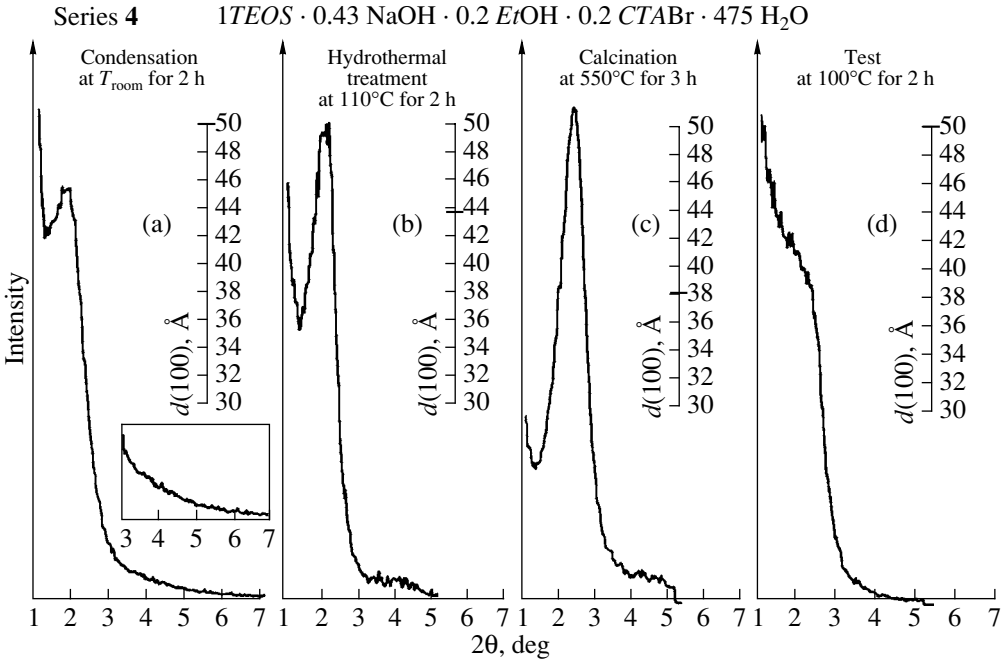

Fig. 5. X-ray diffraction patterns of products of series **4** (see capture to Fig. 2).

ture. Boiling results in a slight degradation of the structure. This manifests itself in an insignificant broadening of the peaks and a decrease in the intensity of far lines.

As can be seen from the X-ray diffraction pattern, the use of the reaction medium without ethanol leads to an increase in the structural inhomogeneity of the condensed product (Fig. 3a). However, the material unquestionably has a hexagonal structure. The (100) line involves a shoulder in the range of small angles, and the (110) and (200) lines become more smeared. These specific features indicate that, apart from the main phase, the product contains a phase that is characterized by a larger lattice parameter and a lower order-

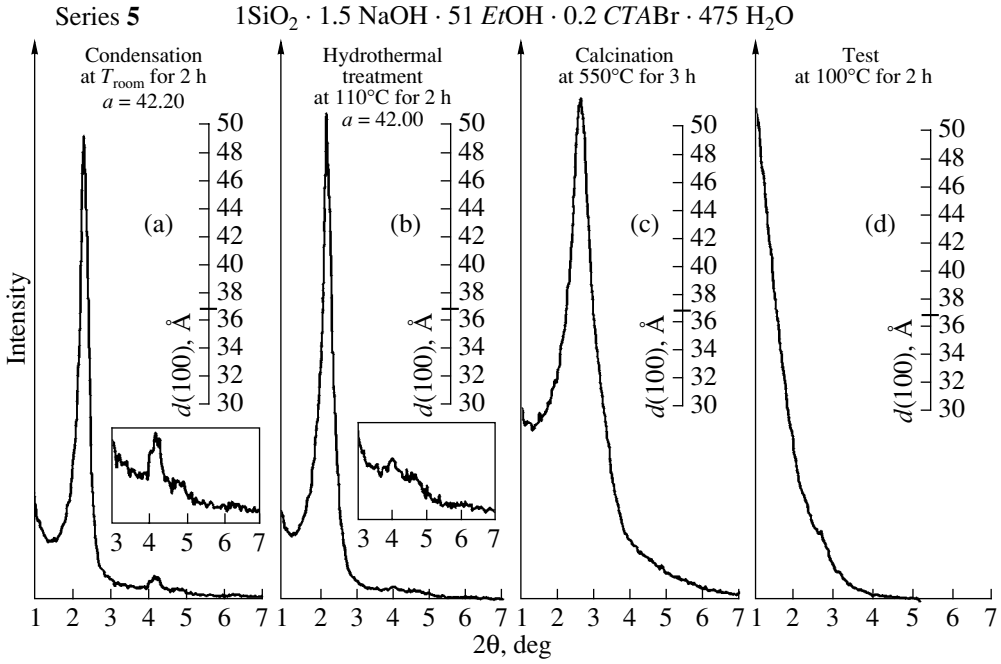

Fig. 6. X-ray diffraction patterns of products of series **5** (see capture to Fig. 2).

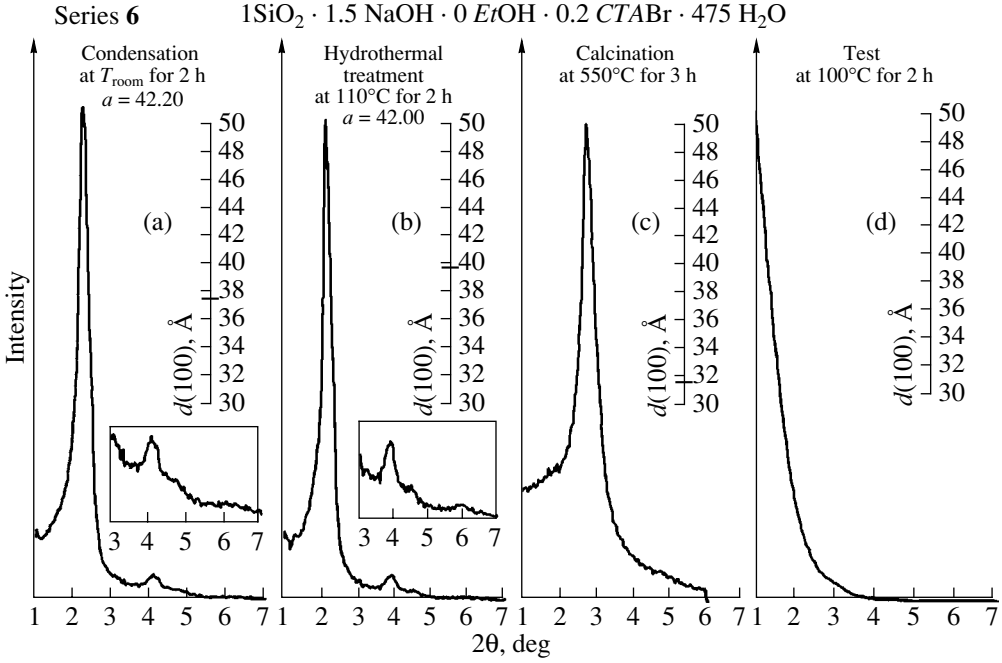

Fig. 7. X-ray diffraction patterns of products of series **6** (see capture to Fig. 2).

ing. Possibly, the inhomogeneous product contains both phases. The unit cell parameter of the main phase is 1.5 Å larger than that of the reference product (Fig. 2a). Judging from the shape of the lines in the X-ray diffraction pattern (Fig. 3b), hydrothermal treatment results in an increase in the degree of crystallinity of the structure. In this case, the lattice parameter increases by 4 Å. The shoulder in the main line in the X-ray diffraction pattern of the condensed product suggests that there were prerequisites for an increase in the lattice parameter. Most likely, this circumstance prevented the transition from the hexagonal phase to the

cubic phase. The result obtained does not confirm the inference made by Romannikov *et al.* [43] that the alcohol serves as a swelling agent, which leads to an increase in the volume (swelling) of the mesophase. After calcination, the lattice parameter also drastically decreases and becomes nearly equal to the initial value. The stability to boiling in water is considerably weaker. In the X-ray diffraction pattern of the material after boiling (Fig. 3d), the primary beam of the diffractometer is broadened noticeably. This suggests the appearances of small-sized particles. Consequently, boiling is attended by breaking initial particles into smaller sized particles.

The effect of the replacement of ammonia as the reagent responsible for the alkalinity of the medium by NaOH in an equivalent amount (initial pH 12.5) is illustrated in Fig. 4. According to Tolbert *et al.* [38], the product already at the condensation stage begins to transform into a form that is intermediate between the MCM-41 and MCM-48 materials and has cubic symmetry. This follows from a decrease in the interplanar distance corresponding to the main diffraction line and the splitting of this line after hydrothermal treatment. A perfect product with cubic symmetry is not formed most likely due to an insufficient time of hydrothermal treatment or other kinetic factors. Subsequent calcination of the product does not result in a more perfect structure that, however, becomes more similar to a cubic structure. The prepared material is unstable upon boiling in water.

At the next step, we decreased the alcohol content in the reaction medium (Fig. 5). This leads to the effect similar to that observed in the second series of experiments, namely, to a decrease in the degree of crystallinity of the primary product due to the insufficient preparation of the surfactant to the reaction. According to the interplanar distance determined from the main reflection (d/n = 49.9 Å), the condensed material can be conventionally assigned to a hexagonal form. A decrease in the ratio d/n to 43.7 Å after hydrothermal treatment corresponds to the onset of the transformation into the cubic phase [38]. Calcination results in a further considerable decrease in the interplanar distance (d/n = 38.1 Å). The final product is not stable to boiling in water.

The influence of the replacement of the silica source was studied in series **5** and **6**. In this case, instead of tetraethoxysilane, we used one more popular silicon-containing compound, namely, the sodium silicate at the ratio Na_2O/SiO_2 = 0.5. The samples of series **5** and **6** (Figs. 6, 7) differ in the presence of ethanol. In series **5**, condensation results in the formation of a rather structured product with hexagonal symmetry. The unit cell parameter (a = 42.2 Å) corresponds to the reference product (series **1**). Hydrothermal treatment results in the onset of the structural transformation (Fig. 6b): the (110) and (200) lines virtually disappear, and the main reflection is shifted toward the large-angle range. Calcination leads to the development of the structural transformation (Fig. 6c). The product loses a mesostructure upon boiling.

A similar behavior is observed in series **6**. The difference lies in a certain time lag as compared to series **5**. After hydrothermal treatment, the product has a more perfect structure with hexagonal symmetry. Note that the lattice parameter increases from 43.2 to 45.4 Å. This is inherent in hexagonal structures. However, a very sharp change in the position of the main line after calcination (from 39.7 to 31.2 Å) indicates that the cubic phase is probably formed. The material is unstable upon boiling in water.

Therefore, the replacement of the reagents leads to substantial changes in the quality of the formed product. Since the final products have the same chemical composition, the observed changes are associated with the changes in the kinetic parameters of individual processes. The results obtained and the role of particular components in these processes can be interpreted by constructing a hierarchy of the main processes occurring during the formation of the material.

At present, many researchers have believed that the main process responsible for the formation of a mesoporous material can be represented by the supramolecular interaction between cetyltrimethylammonium cations and silicate polyanions [7, 10, 11, 15, 19]. The type and size of polyanions are not known.

The careful thermogravimetric investigations performed by Kleitz *et al.* [39] revealed that the weight loss upon calcination of the MCM-41 is somewhat less than 50%. This is in good agreement with our data. According to Jaroniec *et al.* [19], the weight loss during calcination varies from 37 to 42%. Kawi and Shen [26] obtained a weight loss of 53.8%, which in their opinion corresponds to the molar ratio Si/N = 3.79. These data disagree with the inference made by many authors that an excess amount of the surfactant should be used in the synthesis (0.4 M SAA and more per 1 M SiO_2). It should be noted that the same is also true for MCM-48 materials, even though, according to the universally accepted practice [2, 3, 9], they should be synthesized using different proportions of the organic and inorganic components. The above scatter in the thermogravimetric data can be explained by two factors. First, hydrothermal treatment leads to extraction of the surfactant from pores, especially in the case when the pH value is controlled by acids. Second, the polymerization of the silicon–oxygen framework is accompanied by a change in its composition and the loss of water.

The stoichiometry of the SiO_2/SAA ratio is indirectly corroborated by results of investigations into mutual transformations of mesostructured silicate mesophases [38, 40–42]. These results suggest that the cubic structure is formed from the hexagonal phase in the course of hydrothermal treatment.

A large number of works devoted to the search for an optimum ratio of components that can provide the

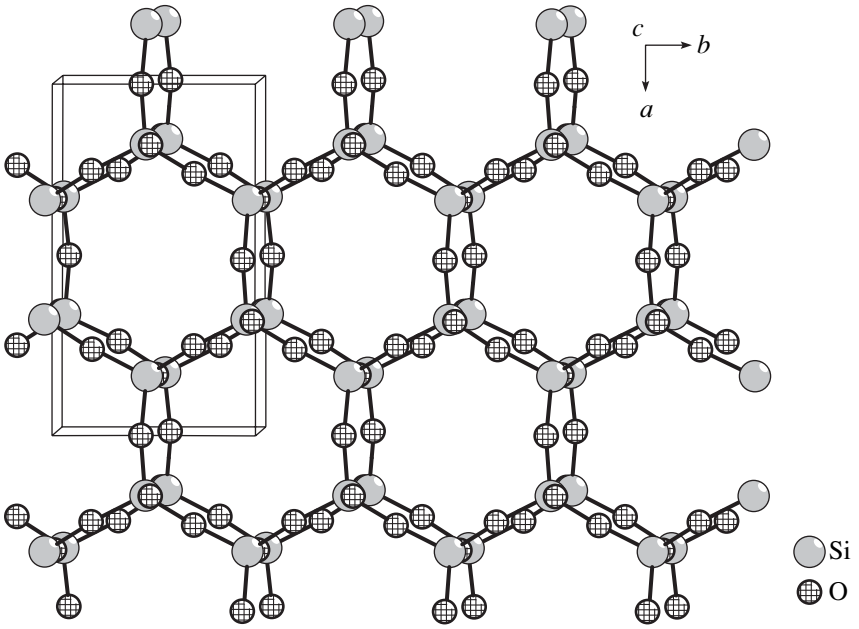

Fig. 8. A bilayer fragment of the SiO_2 tridymite structure.

formation of products with a perfect structure (according to X-ray diffraction patterns) are available in the literature (see, for example, [17, 43, 44]). The analysis of the data obtained demonstrates that the optimum molar ratio SiO_2/SAA falls in the range 4 : 1–6 : 1.

Direct and indirect evidences in favor of this SiO_2/SAA ratio can be found in structural investigations. In many works [23, 34, 36, 37, 45], the authors analyzed geometric structural aspects of materials, such as the thickness and density of pore walls, the size of "heads" of surfactant molecules, and the density of –Si–OH silanol groups on the surface of calcined materials [46]. These quantities, on the whole, correlate well. We estimated the geometric characteristics of pore walls with the use of the tridymite structure (a structural fragment containing two layers, Fig. 8). The estimates show that the density of silanol groups at the points of attachment of surfactant molecules (this corresponds to each fourth silicon atom) is equal to 2.2 nm^{-2}. According to the ^{29}Si NMR data [34, 46], the corresponding density of silanol groups is equal to 2.5–3.0 nm^{-2}. Taking into account that walls involve fractures in which silanol groups can be located, the above densities are in good agreement. The fact that one-fourth of the silicon atoms are bonded to surfactants is confirmed by experiments on silylation of the MCM-41 surface with chloromethylsilane [46], in which it was demonstrated that approximately one-fourth of the silicon atoms transform into the state Q_4 (characterized by four –Si–O–Si bonds).

An important argument in support of the above inference is that a double-layer fragment composed of vertex-shared $[SiO_4]$ tetrahedra and cut from the tridymite structure (Fig. 8) has a thickness of 8.2 Å, which corresponds to the pore wall thickness (8–9 Å) measured by different methods for MCM-41 materials [36, 37]. It should also be noted that the calculated wall density at a characteristic pore volume of 0.8–0.9 cm^3/g agrees well with the tridymite density (2.08 g/cm^3).

In our opinion, similar thicknesses of pore walls in MCM-41 and MCM-48 materials are also associated with the component ratio in initial composites [46, 47]. An excess amount of the surfactant that leads to the formation of the MCM-48 material is the unquestionable experimental fact. However, the corresponding process most likely proceeds through a somewhat different mechanism (see below).

One more feature significant for the analysis of the component ratio is that the highest condensation rate of the material is observed in a limited pH range (11.5–12.5). This can be explained by the highest concentration of polyanions required for condensation. Outside this range, for example, when using the sodium silicate (pH more than 13), the reaction rate is low. Note that an increase in the pH value leads to a decrease in the condensation rate of the solid phase and a decrease in the pH results in the precipitation of an amorphous product.

As follows from the results of *in situ* ^{29}Si NMR investigations into silicate solutions [20], a limited set of silicate anions, among which $[Si_4]$ anions are dominant (the designation reflects the number of silicon atoms in a particle), are formed upon condensation. In these anions, silicon atoms are in the state Q_3 (the silicon atom has three contacts with the nearest silicon atoms).

A good agreement between the density data, a bilayer thickness, and a high degree of connectivity of $[SiO_4]$ tetrahedra suggest that pore walls have a sufficiently ordered structure. It seems likely that the case in point can be only a distortion of the geometrically regular arrangement of $[SiO_4]$ tetrahedra. Although direct data on the arrangement type are absent, the aforementioned bilayer tridymite fragment (Fig. 8) can be treated as a justified model.

Therefore, summing up the foregoing, we can argue with a high degree of confidence that the interaction should occur with components in stoichiometric or close-to-stoichiometric ratios. The corresponding reaction can be described by the following equation:

$$\begin{aligned} &CTA^+ + [Si_4O_{4+x}(OH)_{9-x}]^{-(1+x)} \\ &\longrightarrow CTA[Si_4O_{4+x}(OH)_{9-x}]^{-(x)}. \end{aligned} \quad (1)$$

The value of x lies in the range 0–1 and depends on the pH of the medium. The resulting supramolecular fragments condense (crystallize). The term "self-assembling" used in this situation most likely has the same meaning as the term "crystallization." However, the mechanism of crystallization in the given case involves processes characteristic of constructing an energetically favorable surface (as in liquid crystals), including the spatial orientation of supramolecular fragments embedded in the condensed material. The crystallization mechanism of condensation of the mesostructured material through small-sized fragments, unlike the "micellar" mechanism (through large-sized cylindrical micelles) proposed even in the pioneering works by Beck *et al.* [2, 3], is supported by a regular hexagonal pore shape (Fig. 1c) found in the as-precipitated product in our earlier works [18, 36].

The most probable geometry of the $[Si_4O_{4+x}(OH)_{9-x}]^{-(1+x)}$ polyanion is illustrated in Fig. 9. The "trifolium" shape is very convenient for assembling the wall. On the one hand, an approximate mechanism of incorporation of a small-sized fragment into a growing wall is clear. On the other hand, this provides the formation of a close packing that, in the course of further polymerization, is convenient for forming six-membered rings, which are main structural units of the pore wall. A fragment of the growing wall is depicted in Fig. 10. The described mechanism is hypothetical but is supported by the transformation of the material into the tridymite structure at 1100°C. Finally, back-to-back joining of two silicate trifoliums in the wall can be represented as a step of silica coagulation, which is characteristic of the system under consideration.

The cross-linking of the wall or the silica polymerization is the longest process, which, chemically, can be represented by the equation

$$\equiv Si–OH + HO–Si\equiv \longrightarrow \equiv Si–O–Si\equiv + H_2O. \quad (2)$$

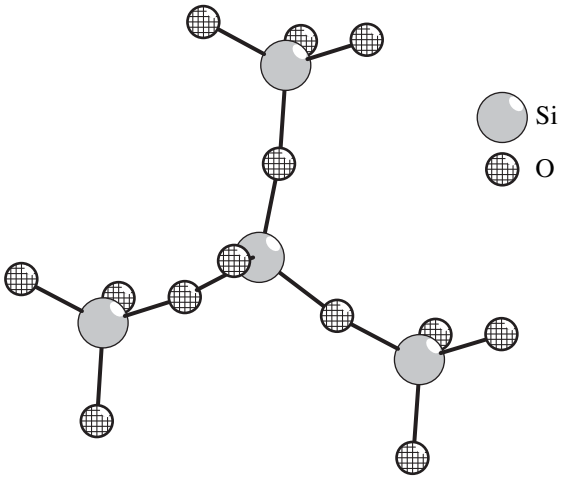

Fig. 9. An $[Si_4O_{10}]$ fragment of the tridymite structure simulating a silicate polyanion.

The main barrier to polymerization is a high charge of the wall as compared to the charge of compensating surfactant cations. Furthermore, a high charge is also responsible for the formation of defects in the arrangement of trifoliums due to repulsion. Highly charged polyanions require neutralization, which is associated with the diffusion of neutralizing agents. Their role can be played by water and ammonium ions. For ammonium ions, the total reaction of neutralization and polymerization can be written in the form of the equation, in which the equilibrium is shifted toward the right; that is,

$$\begin{aligned} &\equiv Si–O^- + HO–Si\equiv + NH_4^+ \\ &\longrightarrow \equiv Si–O–Si\equiv + NH_3 + H_2O. \end{aligned} \quad (3)$$

The sequential processes of neutralization and polymerization of the wall in water are described by the equations

$$\equiv Si–O^- + H_2O \longrightarrow \equiv Si–O–H + OH^-, \quad (4)$$

$$\equiv Si–OH + HO–Si\equiv \longrightarrow \equiv Si–O–Si\equiv + H_2O. \quad (5)$$

In this case, it is suggested that sodium cations (or other counterions), which neutralize the wall charge, are located in the vicinity of the wall. Since a strong base is formed in the reaction zone, the hydrolysis process is reversible and the polymerization rate becomes lower. A decrease in the polymerization rate is also favored by hindered diffusion of sodium and hydroxide ions from channels of the mesoporous material and also by purely geometrical (steric) factors, which will be considered below.

The presence of sodium ions in pores can cause an osmotic effect. The charge of the silicate framework of the material is distributed over the surface. Since the inner surface area is larger than the outer surface area (sometimes, by a factor of several tens), the corre-

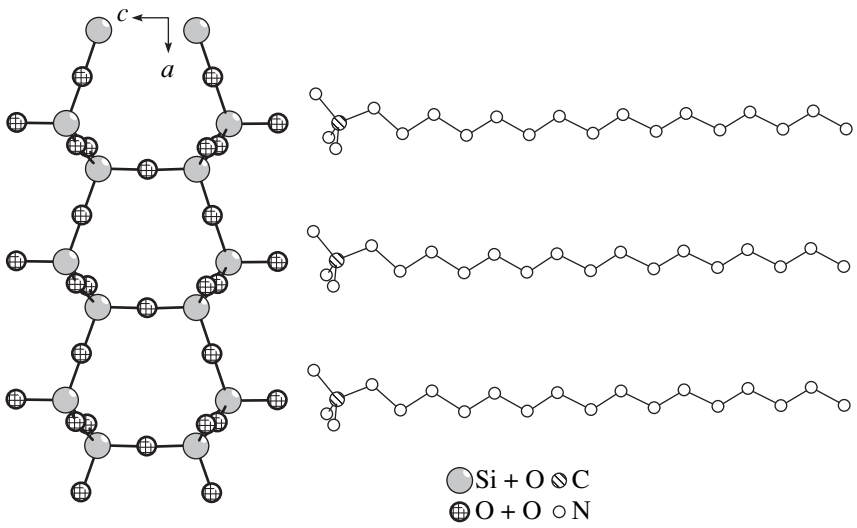

Fig. 10. Model of the wall (perpendicular section) illustrating the orientation of surfactant ions with respect to the pore wall in the organosilicate composite.

sponding number of compensating counterions should be located inside pores. This leads to the redistribution of ions in the system. A part of the charge according to the stoichiometry is compensated for by surfactants, and the other charge should be compensated for by ammonium or sodium cations. If the ratio of the initial components results in the situation when, for example, the concentration of sodium ions inside pores is higher than that in the reaction solution, heating can induce the osmotic pressure within pores. The osmotic pressure can not only increase the pore size but also lead to the structural transformation of the material. The osmotic pressure can be induced by ammonium and excess surfactant ions. The use of salt additives for improving the hydrothermal stability of materials is described in the literature [27, 30–33]. It was revealed that introduction of additional sodium ions in the reaction solution after phase precipitation (but before hydrothermal treatment) leads to an increase in the stability of the material. This can be easily explained within the osmotic hypothesis: excess sodium ions decrease disbalance of their concentrations outside and inside pores.

Sodium ions are very strong transforming agents with respect to the structure. They have a double effect. On the one hand, these ions hinder polymerization of the framework of the material and remain it in a mobile state. On the other hand, sodium ions induce the osmotic pressure of the solution inside pores. A positive effect of the osmosis manifests itself in the ordering of pores and equalization of their size. In particular, this reflects in a higher quality of the X-ray diffraction pattern of the product after hydrothermal treatment. A negative effect manifests itself in a too strong expansion of pores. The lattice parameter increases by several angstroms. The expansion is caused by the local elongations of the wall in regions that do not undergo cross-linking (polymerization). In these regions, the distances between polysilicate anions become so large that there arise spatial hindrances to polymerization. The described phenomenon is characteristic of the experiments in series **3**–**6**.

The proposed scheme of the processes permits us to find the reasonable explanation for the results obtained and the role of each reagent used in these processes.

The alcohol (ethanol) in the process serves as a solvent of the surfactant rather than as a swelling agent. It should be remembered that, when the surfactant is in excess, there arises a phenomenon similar to osmosis in nature but associated with the alcohol. A relatively small addition of ethanol to the aqueous solution of the surfactant leads to the complete dissolution of cetyltrimethylammonium bromide. As a consequence, the surfactant turns out to be better prepared to the interaction with silica. It is apparent that this is ensured by solvation of organic components of surfactant molecules. It is interesting to note that, upon a considerable increase in the alcohol concentration, the surfactant–alcohol liquid phase begins to precipitate from the aqueous solution.

In series **2**, as was noted above, the inhomogeneous material is formed in the absence of the alcohol. In this case, the formation of the phase is due to crystallization of normal aggregates and also aggregates in which bound surfactant molecules are solvated by “free” surfactant molecules. There is a probability that the latter aggregates initially crystallize with the formation of a distorted lattice. Then, normal aggregates crystallize on these grains. During hydrothermal treatment, surfactant molecules nonbonded to walls are redistributed over channels, resulting in a substantial expansion of pores. This expansion leads to the formation of fractures in

walls and, eventually, to a decrease in the stability of the material.

In series **3** and **4**, we observed the influence of replacement of the alkali agent. Although the alkali does not enter into the composition of the final product and the alkalinity (acidity) is maintained at the same level, the alkali agent has a very substantial effect. Hydrolysis of tetraethoxysilane, unlike sodium silicate, rapidly leads to the formation of well-arranged silicate polyanions suitable for the interaction with the surfactant. This is associated with the kinetic characteristics and the path of the process, which begins with individual silicate anions. When using the strong alkali agent, polyanions have a high charge. This circumstance manifests itself at the first stage of the product formation; as a result, the material has a tendency to the transformation into the cubic phase. As the sodium hydroxide content decreases with respect to SiO_2 (series **4**), it follows from the interplanar distance corresponding to the main line that the product after condensation is more similar to a phase with a hexagonal structure. However, already in the course of hydrothermal treatment, the material starts to transform into the phase with cubic symmetry [38]. In both cases, the synthesis time appears to be insufficient for completing the process. An increase in the time that it takes for the process to be completed is caused by the decrease in the hydrolysis rate in the case of strong alkali agents. Since the formation of products is not completed, their structure is characterized by a low degree of polymerization and, correspondingly, by a low hydrothermal stability.

If instead of tetraethoxysilane (series **3**, **4**), sodium silicate (series **5**, **6**) serves as the silicon source, the equilibrium between the species of dissolved silica is reestablished more slowly after exhausting Si_4 species for the formation of the mesoporous product because of the aforementioned difference between the hydrolysis rates. Therefore, the formation rate of the mesoporous materials becomes slower. As a result, the condensation process is completed at the stage of forming the hexagonal phase. However, a further evolution during hydrothermal treatment proceeds toward the transformation into the product with the cubic structure. The evolution of the material in series **5** leads the evolution of the material in series **6**, in which ethanol is absent in the initial reaction mixture. In the latter case, the excess amount of the surfactant in pores most likely goes to neutralize the inner surface, which retards the structural transformation.

CONCLUSIONS

Thus, the formation of a mesostructured mesoporous material is due to a number of processes that differ in the onset and the rate. At preliminary stages, silicate polyanions with a necessary shape arise and the surfactant dissolves with the formation of individual anions. Then, supramolecular particles are formed in silicate polyanion–surfactant cation complexes. Thereafter, the particles condense to a mesophase. Hydrolysis and polymerization of the inorganic component occur in the mesophase. Hydrothermal treatment has a twofold effect. On the one hand, this treatment promotes the polymerization processes. On the other hand, if there are conditions for osmosis, hydrothermal treatment initially results in the expansion (equalization) of pores and, at a high osmotic pressure, the expansion can be so large that polymerization is retarded or completely terminated due to geometric hindrances. When osmotic processes lead polymerization, the material transforms into the phase with a cubic structure. The reagents used affect the rate of the processes. Ethanol participates in the dissolution of the surfactant. The alkali agents provide the hydrolysis, polymerization, and osmosis processes.

ACKNOWLEDGMENTS

This work was supported by the International Association of Assistance for the Promotion of Cooperation with Scientists from the New Independent States of the Former Soviet Union (project INTAS no. 01-2283), the Russian Foundation for Basic Research (project no. 03-03-32127), and the Krasnoyarsk Regional Science Foundation (project RFFI–KKFN no. 02-03-97706).

REFERENCES

1. Iler, R.K., *Chemistry of Silica*, New York: Wiley, 1979.
2. Kresge, C.T., Leonowicz, M.E., Roth, W.J., *et al.*, Ordered Mesoporous Molecular Sieves Synthesized by a Liquid-Crystal Template Mechanism, *Nature* (London), 1992, vol. 359, pp. 710–712.
3. Beck, J.S., Vartuli, J.C., Roth, W.J., *et al.*, A New Family of Mesoporous Molecular Sieves Prepared with Liquid Crystal Templates, *J. Am. Chem. Soc.*, 1992, vol. 114, pp. 10834–10843.
4. Yanagisawa, T., Shimizu, T., Kuroda, K., and Kato, C., The Preparation of Alkyltrimethylammonium-Kanemite Complexes and Their Conversion to Microporous Materials, *Bull. Chem. Soc. Jpn.*, 1990, vol. 63, pp. 988–992.
5. US Patent 2810902 (Du Pont), 1957 (cited according to [1]).
6. Chiola, V., Ritsko, J.E., and Vanderpool, C.D., Process for Producing Low-Bulk Density Silica, US Patent 3556725, 1971.
7. Stucky, G.D., Monier, A., Schuth, F., *et al.*, Molecular and Atomic Arrays in Nanoporous Materials Synthesis, *Mol. Cryst. Liq. Cryst.*, 1994, vol. 240, pp. 187–200.
8. Zhao, X.S., Lu, G.Q., and Mullar, G.J., Advances in Mesoporous Molecular Sieve MCM-41, *Ind. Eng. Chem. Res.*, 1996, vol. 35, pp. 2075–2090.
9. Vartuli, J.C., Kresge, C.T., Roth, W.J., *et al.*, Designed Synthesis of Mesoporous Molecular Sieve Systems Using Surfactant Directing Agents, in *Advanced Catalysts and Nanostructured Materials: Modern Synthetic Methods*, Moser, W., Ed., San Diego: Academic, 1996.

10. Biz, S. and Occelli, M.L., Synthesis and Characterization of Mesostructured Materials, *Catal. Rev.–Sci. Eng.*, 1998, vol. 40, no. 3, pp. 329–407.
11. Ciesla, U. and Schuth, F., Ordered Mesoporous Materials, *Micropor. Mesopor. Mater.*, 1999, vol. 27, pp. 131–149.
12. Davis, M.E., Ordered Porous Material for Emerging Applications, *Nature* (London), 2002, vol. 417, pp. 813–821.
13. Schuth, F. and Schmidt, W., Microporous and Mesoporous Materials, *Adv. Eng. Mater.,* 2002, vol. 4, no. 5, pp. 269–279.
14. Corma, A., From Microporous to Mesoporous Molecular Sieve Material and Their Use in Catalysis, *Chem. Rev.,* 1997, vol. 97, pp. 2373–2419.
15. Hayward, R.C., Alberius-Henning, P., Chmelka, B.F., and Stucky, G.D., The Current Role of Mesostructures in Composite Materials and Device Fabrication, *Micropor. Mesopor. Mater.*, 2001, vols. 44–45, pp. 619–624.
16. Soler-Illia, G.J. de A.A., Sanchez, C., Lebeau, B., and Patarin, J., Chemical Strategies to Design Textured Materials: From Microporous and Mesoporous Oxides to Nanonetworks and Hierarchical Structures, *Chem. Rev.*, 2002, vol. 102, pp. 4093–4138.
17. Romannikov, V.N., Fenelonov, V.B., Nosov, A.V., *et al.*, Physicochemical Features of Formation of Silicate Porous Mesophases: I. General Concepts of Mechanism, *Izv. Akad. Nauk, Ser. Khim.*, 1999, no. 10, pp. 1845–1851.
18. Solovyov, L.A., Kirik, S.D., Shmakov, A.N., and Romannikov, V.N., A Continuous Electron Density Approach in Rietveld Analysis for Structure Investigations of the Mesoporous Silicate Materials, *Adv. X-ray Anal.*, 2001, vol. 44, pp. 110–115.
19. Jaroniec, M., Kruk, M., Shin, H.J., *et al.*, Comprehensive Characterization of Highly Ordered MCM-41 Silicas Using Nitrogen Adsorption, Thermogravimetry, X-ray Diffraction, and Transmission Electron Microscopy, *Micropor. Mesopor. Mater.*, 2001, vol. 48, pp. 127–134.
20. McCormick, A.V. and Bell, A.T., The Solution Chemistry of Zeolite Precursors, *Catal. Rev.–Sci. Eng.*, 1989, vol. 31, pp. 97–118.
21. Grun, M., Unger, K.K., Matsumoto, A., and Tsutsumi, K., Novel Pathways for the Preparation of Mesoporous MCM-14 Materials: Control of Porosity and Morphology, *Micropor. Mesopor. Mater.*, 1999, vol. 27, pp. 207–216.
22. Di Renzo, F., Testa, F., Chen, J.D., *et al.*, Textural Control of Micelle-Templated Mesoporous Silicates: The Effects of Co-Surfactants and Alkalinity, *Micropor. Mesopor. Mater.,* 1999, vol. 28, pp. 437–446.
23. Schulz-Ekloff, G., Rathousky, J., and Zukal, A., Controlling of Morphology and Characterization of Pore Structure of Ordered Mesoporous Silica, *Micropor. Mesopor. Mater.*, 1999, vol. 27, pp. 273–285.
24. Yu, J., Shi, J.-L., Wang, L.-Z., *et al.*, Preparation of High Thermal Stability MCM-41 in the Low Surfactant/Silicon Molar Ratio Synthesis System, *Mater. Lett.*, 2001, vol. 48, pp. 112–116.
25. Kruk, M., Jaroniec, M., and Sayari, A., Influence of Hydrothermal Restructuring Conditions on Structural Properties of Mesoporous Molecular Sieves, *Micropor. Mesopor. Mater.*, 1999, vol. 27, pp. 217–229.
26. Kawi, S. and Shen, S.-C., Effects of Structural and Non-Structural Al Species on the Stability of MCM-41 Materials in Boiling Water, *Mater. Lett.*, 2000, vol. 42, pp. 108–112.
27. Kim, W.J., Yoo, J.C., and Hayhurst, D.T., Synthesis of Hydrothermally Stable MCM-41 with Initial Adjustment of pH and Direct Addition of NaF, *Micropor. Mesopor. Mater.*, 2000, vol. 39, pp. 177–186.
28. Kisler, J.M., Gee, M.L., Stevens, G.W., and O'Connor, A.J., Comparative Study of Silylation Methods to Improve the Stability of Silicate MCM-41 in Aqueous Solutions, *Chem. Mater.*, 2003, vol. 15, pp. 619–624.
29. Mokaya, R., Influence of Alumination Pathway on the Steam Stability of Al-Grafted MCM-41, *Stud. Surf. Sci. Catal.*, 2003, vol. 146, pp. 435–438.
30. Kim, W.J., Yoo, J.C., and Hayhurst, D.T., Synthesis of MCM-48 via Phase Transformation with Direct Addition of NaF and Enhancement of Hydrothermal Stability by Post-Treatment in NaF Solution, *Micropor. Mesopor. Mater.*, 2001, vol. 49, pp. 125–137.
31. Kim, J.M., Jun, S., and Ryoo, R., Improvement of Hydrothermal Stability of Mesoporous Silica Using Salts: Reinvestigation for Time-Dependent Effects, *J. Phys. Chem. B*, 1999, vol. 103, pp. 6200–6205.
32. Lin, H.-P. and Mou, C.-Y., Salt Effect in Post-Synthesis Hydrothermal Treatment of MCM-41, *Micropor. Mesopor. Mater.*, 2002, vol. 55, pp. 69–80.
33. Oye, G., Sjoblom, J., and Stocker, M., Synthesis and Characterization of Siliceous and Aluminum-Containing Mesoporous Materials from Different Surfactant Solutions, *Micropor. Mesopor. Mater.*, 1999, vol. 27, pp. 171–180.
34. Zhao, X.S. and Lu, G.Q., Modification of MCM-41 by Surface Silylation with Trimethylchlorosilane and Adsorption Study, *J. Phys. Chem. B*, 1998, vol. 102, pp. 1556–1561.
35. Lee, J.S., Joo, S.H., and Ryoo, R., Synthesis of Mesoporous Silicas of Controlled Pore Wall Thickness and Their Replication to Ordered Nanoporous Carbons with Various Pore Diameters, *J. Am. Chem. Soc.*, 2002, vol. 124, no. 7, pp. 1156–1157.
36. Solovyov, L.A., Kirik, S.D., Shmakov, A.N., and Romannikov, V.N., X-ray Structural Modeling of Mesoporous Mesophase Material, *Micropor. Mesopor. Mater.*, 2001, vols. 44–45, pp. 17–23.
37. Fenelonov, V.B., Derevyankin, A.Yu., Kirik, S.D., *et al.*, Comparative Textural Study of Highly Ordered Silicate and Aluminosilicate Mesoporous Mesophase Materials Having Different Pore Sizes, *Micropor. Mesopor. Mater.*, 2001, vols. 44–45, pp. 33–40.
38. Tolbert, S.H., Landry, C.C., Stucky, G.D., *et al.*, Phase Transitions in Mesostructured Silica/Surfactant Composites: Surfactant Packing and Role of Charge Density Matching, *Chem. Mater.*, 2001, vol. 13, pp. 2247–2256.
39. Kleitz, F., Schmidt, W., and Schuth, F., Evolution of Mesoporous Materials during the Calcination Process: Structural and Chemical Behavior, *Micropor. Mesopor. Mater.*, 2001, vols. 44–45, pp. 95–109.

40. Gallis, K.W. and Landry, C.C., Synthesis of MCM-48 by a Phase Transformation Process, *Chem. Mater.*, 1997, vol. 9, pp. 2035–2046.
41. Xu, J., Luan, Z.H., He, H.Y., *et al.*, A Reliable Synthesis of Cubic Mesoporous MCM-48 Molecular Sieve, *Chem. Mater.,* 1998, vol. 10, pp. 3690–3698.
42. Pevzner, S. and Regev, O., The *In Situ* Phase Transitions Occurring during Bicontinuous Cubic Phase Formation, *Micropor. Mesopor. Mater.*, 2001, vol. 38, pp. 413–421.
43. Romannikov, V.N., Fenelonov, V.B., and Derevyankin, A.Yu., Physicochemical Features of Formation of Silicate Porous Mesophases: II. The Effect of Size of Molecules of Surfactant Cations, *Izv. Akad. Nauk, Ser. Khim.*, 1999, no. 10, pp. 1852–1856.
44. Kodenev, E.G., Shmakov, A.N., Derevyankin, A.Yu., *et al.*, Physicochemical Features of Formation of Silicate Porous Mesophases: III. Conditions of Formation and Properties of Mesoporous Silica, *Izv. Akad. Nauk, Ser. Khim.*, 2000, no. 10, pp. 1685–1691.
45. Zhao, X.S., Lu, G.Q., Whittaker, A.K., *et al.*, Comprehensive Study of Surface Chemistry of MCM-41 Using Si-29 CP/MAS NMR, FTIR, Pyridine-TPD, and TGA, *J. Phys. Chem. B*, 1997, vol. 101, pp. 6525–6531.
46. Solovyov, L.A., Belousov, O.V.., Shmakov, A.N., *et al.*, X-ray Diffraction Analysis of Mesostructured Materials by Continuous Density Function Technique, *Stud. Surf. Sci. Catal.*, 2003, vol. 146, pp. 299–302.
47. Solovyov, L.A., Zaikovskii, V.I., Shmakov, A.N., *et al.*, Framework Characterization of Mesostructured Carbon CMK-1 by X-ray Powder Diffraction and Electron Microscopy, *J. Phys. Chem. B*, 2002, vol. 106, pp. 12 198–12 202.